Numerical De-embedding of Periodic Guided-wave Structures via SOL/SOC in FEM Algorithm

Yin Li, Danpeng Xie, and Lei Zhu

Department of Electrical Engineering
University of Macau, Macau, 519000, SAR, China
yb57430@connect.umac.mo, yb57471@umac.mo, LeiZhu@umac.mo

Abstract ─ This paper presents a 3D full-wave finite element method (FEM) combined with short-open-load (SOL) and short-open calibration (SOC) technique. Due to the effective calibration of the port discontinuities between the feeding line and periodic structure, both SOL and SOC can successfully extract the intrinsic unite-length parameters, i.e., complex propagation constants and effective characteristic impedances. Distinctively, the SOL can be easily implemented with the commercial software such as Ansys HFSS, which is widely applicable for various kinds of periodic structure. More importantly, the SOC incorporated within the FEM algorithm intrinsically reduces the requirement of the load standard in SOL. Also, the SOC in FEM will be independent with the absorbing boundary condition at the port. And the port information such as characteristic impedance and propagation constants at the designated port will not be required in advanced, thereby allowing the arbitrary implementation of non-uniform feeding structures. In order to demonstrate the efficiency and accuracy of our proposed approaches, two numerical examples are given out for verification.

Index Terms ─ Characteristic impedances, finite element method, periodic structures, port discontinuities, short-open calibration, short-open-load.

I. INTRODUCTION

Recently, a great demand for full-wave modeling and characterization of the integrated and multifunctional microwave and millimeter-wave circuits has been rapidly grown. Especially for a large number of designs with various types of periodic structures, including substrate integrated waveguide (SIW) [1], air-filled substrate integrated waveguide (AFSIW) [2-4] and metamaterials [5], etc., the high-accuracy and high-efficiency modeling approach for their guided-wave characterization become significantly important.

A traditional approach based on the Floquet theory utilizes the eigenvalue of the unit cell to characterize the infinite periodic structure [6]. However, it becomes extremely time-consuming and low-efficient when solving the eigenvalue problem of each unit cell. Although eigenmode solver has been implemented into commercial software, such as Ansys HFSS [7] and CST Microwave Studio [8], the attenuation constant and the characteristic impedance of the periodic structures still cannot be directly extracted. In this way, only the phase constant of the periodic structures can be acquired through the eigenvalue solver.

In practice, the unit cell of the periodic structure is commonly considered as an equivalent two-port network, hence the propagation characteristics of the periodic structures can be easily retrieved by the network parameters. As for realization, the port models such as lumped port and wave port are widely used to conveniently excite the two-port network. However, the lumped port models introduce an undesired port discontinuity [9, 10], due to the inaccurate description of the field at the port. Even though the wave port model can describe the filed by solving the eigenvalue problem of the cross-section at the port [11-13], the discontinuity between the feeding line and the periodic structure still exists. It will unavoidably bring in certain inaccuracy, resulting from the reflected waves back to the port [1].

Thereafter, calibration methods are accordingly conducted during the numerical modeling, aiming at the elimination of the above-described discontinuities. The so-called "double-delay de-embedding" was developed to estimate and remove out the port discontinuity [10, 14, 15]. Inspired by the calibration procedure in measurement, the numerical thru-reflect-line (TRL) calibration method was developed to effectively model the SIW devices [16, 17]. Moreover, the thru-line (TL) calibration method was also proposed for the extraction of the SIW structures [1, 18, 19]. Similarly, the through-resistor (TR) calibration method was proposed to de-embed the port discontinuities [20]. In addition, the even-odd-mode excitation was employed to analyze the port discontinuity for accurate modeling [21]. Despite that, individual limitations regarding each of the above calibration methods restrict their applicability. For

Submitted On: October 12, 2018
Accepted On: December 9, 2018

example, double-delay method needs to pre-define the format of the port discontinuities as shunt impedance, and two feeding lines in TL method must be symmetrically implemented. Electrical lengths between the line-standard and thru-standard should be determined according to the operation frequency, and the whole procedure needs to be carried out within a certain bandwidth.

As is well known, the short-open-calibration (SOC) technique was first proposed in 1997 [9], which is capable to accurately and efficiently estimate the error box by only a pair of calibration standards, named as ideal short- and open-end. It has been applied to extract the equivalent model parameters of planar circuit elements [9]. The port discontinuity and its respective feeding line are considered as an error box. After removing it out, the characteristic parameters of the periodic structures, such as coplanar waveguide (CPW) electromagnetic bandgap (EBG) [22] and CPW metamaterial structures [23], are accurately extracted.

The short-open-load (SOL) technique has been recently integrated into the 3D commercial full-wave simulator HFSS (HFSS-SOL) [24, 25, 26]. By virtue of the short, open and load standards, the periodic structures with 3D cell can be conveniently and accurately analyzed. However, the port information needs to be known or calculated in advance, whereas the realization of a load standard is usually difficult to implement. Therefore, in order to avoid the load standard element, the SOC method is further implemented in the 3D finite-element method (FEM) algorithm (FEM-SOC). It requires completely no absorbing boundary condition at the port. Also, the pre-knowledge of the port information is not needed at all. In [27], the feeding line and the port discontinuity are considered as the error box, so the characteristic parameters of the periodic structures can be extracted. In this work, two numerical examples, i.e., an AFSIW guided-wave structure modeled by HFSS-SOL and a non-uniformly-fed pin-loaded microstrip line analyzed by FEM-SOC are separately exhibited and demonstrated. In addition, the effect of the non-uniform feeding structures is discussed.

II. SOL AND SOC TECHNIQUE IN FEM

As shown in Fig. 1 (a), the equivalent circuit model of the periodic structure with *N*–unit cells fed by a pair of sources at two sides is exhibited. The longitudinal dimension of the core *N*–unit cells is $L = N \times T$, where T is the periodicity of each unit cell. The core circuit of the periodic structure can be equivalent to a uniform transmission line, whose effective guided-wave parameters include the complex propagation constant and characteristic impedance. The core circuit can be excited by the impressed source with the feeding line and port discontinuity as shown in the Fig. 1 (b).

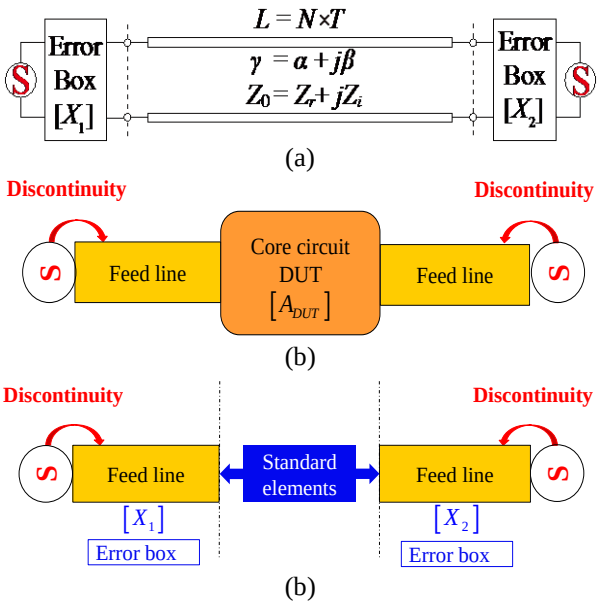

Fig. 1. Equivalent circuit model of periodic structure fed by impressed sources at two ports and its calibration process.

As shown in Fig. 1 (c), the feeding line and port discontinuity are included into the error box, which can be estimated by the standard elements and then removed out. And then, the accurate results of the core circuit can be obtained. For both SOC and SOL techniques, the feeding line and the port discontinuity are included in the two error boxes, which need to be evaluated, thus to be removed out for accurate extraction of the periodic structure. According to different calibration standards, distinctive de-embedding procedures between the SOL and SOC techniques are respectively implemented.

A. SOL de-embedding technique

As for SOL de-embedding technique, three standard elements, including short, open, and load standards, are explicitly depicted in Fig. 2. These three standards can be respectively realized by three kinds of boundary conditions, i.e., perfect electric conductor (PEC), perfect magnetic conductor (PMC), and matched load. They can be easily realized in full-wave simulator.

In terms of the error box [*X*], the four elements of its ABCD-matrix are defined as *a*, *b*, *c*, *d*. By using the transmission line theory, the input impedance for the error box loaded with the impedance Z_L can be expressed as:

$$Z_{in} = \frac{a * Z_L + b}{c * Z_L + d}. \tag{1}$$

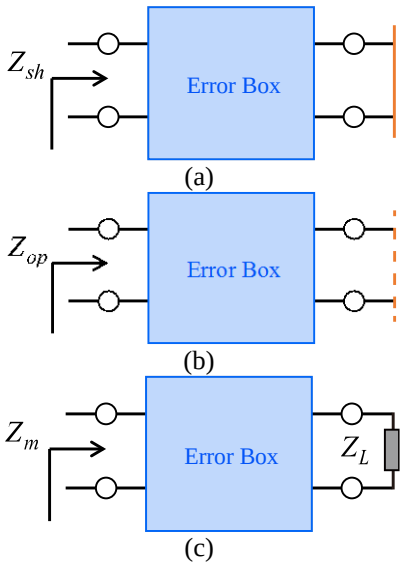

Fig. 2. The three calibration standards in SOL technique: (a) short standard, (b) open standard, and (c) load standard.

For the short-circuited element (Z_L = 0), the input impedance (Z_{sh}) can be written as:

$$Z_{sh} = \frac{b}{d}. \tag{2}$$

For the open-circuited element (Z_L = ∞), the input impedance (Z_{op}) can be written as:

$$Z_{op} = \frac{a}{c}. \tag{3}$$

For the matched-load element (Z_L = Z_m), the input impedance (Z_m) can be written as:

$$Z_m = \frac{a * Z_m + b}{c * Z_m + d}. \tag{4}$$

Since the error box is a two-port reciprocal network, an additional equation can be written as:

$$a*d - b*c = 1. \tag{5}$$

By solving the equations (1)-(5), the ABCD-matrix of the error box can be expressed as:

$$\begin{bmatrix} a & b \\ c & d \end{bmatrix} = \begin{bmatrix} cZ_{op} & \dfrac{Z_{sh}}{c\left(Z_{op} - Z_{sh}\right)} \\ c & \dfrac{1}{c\left(Z_{op} - Z_{sh}\right)} \end{bmatrix}. \tag{6}$$

Where:

$$c = \frac{\sqrt{Z_{sh} - Z_m}}{\sqrt{Z_m (Z_m - Z_{op})(Z_{op} - Z_{sh})}}. \tag{7}$$

B. SOC de-embedding technique

Different from the SOL technique, only the short and open standards are needed in SOC de-embedding process. The network parameters of *i-th* (i = 1, 2) error box can be modeled in terms of the FEM-calculated equivalent voltages, expressed as [28]:

$$[X_i] = \begin{bmatrix} \dfrac{\bar{V}_{io}' \bar{V}_{is}}{\bar{V}_{io} - \bar{V}_{is}} & -\dfrac{\bar{V}_{io}' \bar{V}_{is}}{\bar{V}_{io} - \bar{V}_{is}} \\ -\dfrac{1}{\bar{V}_{io}'} & \dfrac{\bar{V}_{io}'}{\bar{V}_{io}'} \end{bmatrix}. \tag{8}$$

Finally, by removing the ABCD-matrix of the error boxes from the whole cascading network, the desired ABCD-matrix of the core circuits can be derived. These two calibration methods are effective and efficient to estimate the ABCD matrix of the error boxes. Subsequently, the effective characteristic impedance and complex propagation constants of the discussed periodic structure can be calculated in terms of the obtained ABCD matrix (with elements a_p, b_p, c_p, d_p), such that:

$$\cosh(\gamma L) = \frac{a_p + d_p}{2}, \tag{9}$$

$$Z_0 = \sqrt{\frac{b_p}{c_p}}. \tag{10}$$

III. NUMERICAL EXAMPLES

A. Modeling of AFSIW by using HFSS-SOL

The AFSIW has advanced features such as low-loss and high power-handling capability, which can be widely used to design various kinds of microwave and millimeter wave components [2-4]. As demonstrated in Fig. 3, the cross-sectional view and top view of the AFSIW geometry are clearly shown. Different from the conventional SIW structure, the central region within the upper and lower conductor layers is partially removed out. The distance between the two rows of the metallic via-holes is W1, and the width of the air-filled region is W2. The dimension of the via-hole is d and the periodicity of the shorting via is T. Herein, the dielectric substrate Arlon AD255A with relative permittivity of ε_r = 2.55, dielectric loss tangent of tanδ = 0.0015, the height of h = 0.5 mm is selected into the design prototype.

As depicted in Fig. 4, the dispersion diagram of the AFSIW under the different air-filled ratios of W2/W1 illustrates the unique dispersive variations of the phase and attenuation constants. In order to inherently acknowledge the attenuation constant variation, here during the simulation, only the dielectric loss is brought into the modeling, without considering the conductor loss. As can be seen in Fig. 4 (a), as the air-filled region is gradually extended with *W2*/*W1* = 0.8, the attenuation constant generated by the dielectric loss is obviously reduced lower than the value of 0.1. This phenomenon validates the low-loss feature caused by the air-filled

configuration of the AFSIW structure. As further shown in Fig. 4 (b), the cut-off frequency of AFSIW as a function of the varied air-filled ratios is obtained. Also, the real and imaginary part of the characteristic impedances under different air-filled ratios are accurately extracted, as exhibited in Figs. 5 (a) and (b), respectively.

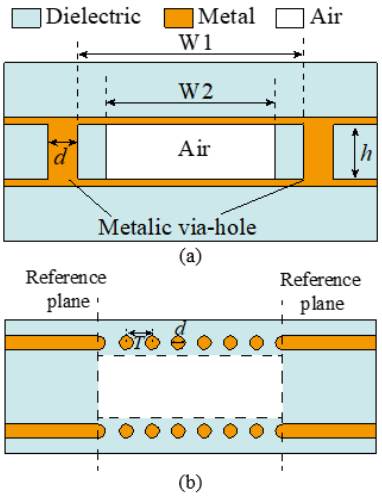

Fig. 3. The geometry of AFSIW: (a) cross-sectional view, and (b) top view of AFSIW with the feeding structures.

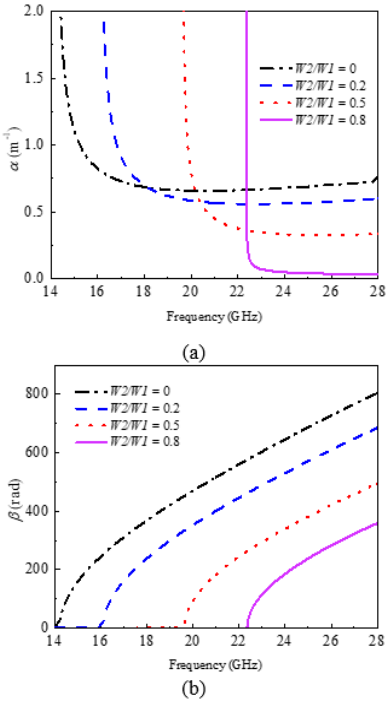

Fig. 4. The dispersion curves of the AFSIW under different dimensions of the air-filled region: (a) attenuation constant, and (b) propagation constant.

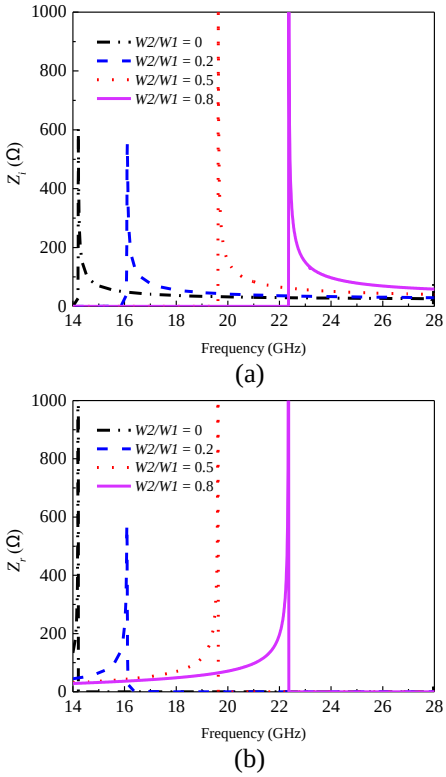

Fig. 5. The extracted characteristic impedance of the AFSIW under different dimensions of the air-filled region: (a) real part and (b) imaginary part.

B. Pin-loaded microstrip line modeled by FEM-SOC

Geometry of the microstrip line with periodical loading of shorting pins is detailly expressed in Fig. 6 (a). Here, the dielectric substrate with relative permittivity of ε_r = 2.65 and height of h = 3.0 mm is selected into the design. The key dimensional parameters of the discussed pin-loaded microstrip line are d = 1.6 mm, T = 15.0 mm, and W = 15.0 mm.

Superiorly, the FEM-SOC does not require the absorbing boundary condition at the port, and the pre-knowledge of the port information is also exempted. Thereby, arbitrary non-uniform feeding structures can be utilized for de-embedding. Here in Fig. 6 (b), two types of feeding mechanisms are used to excite the periodic structure, i.e., Case I with the uniform feeding line and Case II with the non-uniform feeding line.

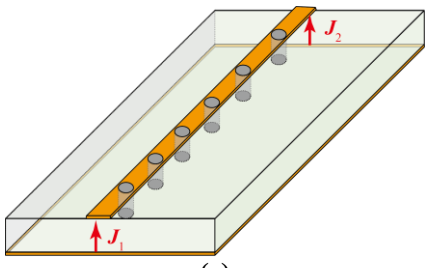

(a)

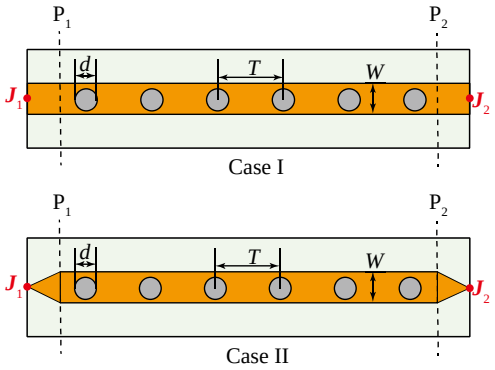

(b)

Fig. 6. Geometry of the microstrip line with the periodic shorting pins: (a) 3D view and (b) top view of the microstrip line with the periodic shorting pin with different feeding mechanisms: Case I with the uniform feeding line; Case II with the non-uniform feeding line.

As verified in Fig. 7, even if the non-uniform feeding mechanism is used, the extracted complex propagation constants and effective characteristic impedance are still remaining in good accordance with the uniform case, which reveals the strong robustness of the proposed FEM-SOC.

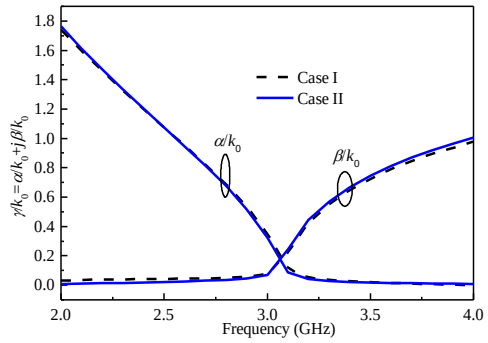

(a)

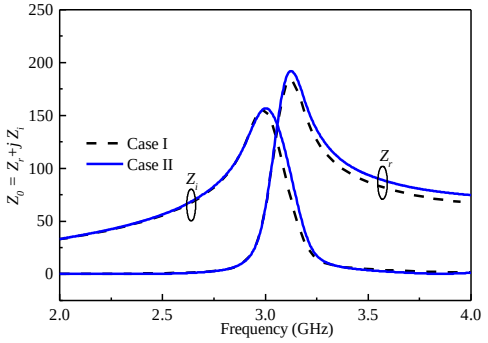

(b)

Fig. 7. The extracted parameters of the pin-loaded microstrip line under different feeding mechanisms: (a) complex propagation constants, and (b) effective characteristic impedance.

V. CONCLUSION

In this paper, de-embedding and modeling of periodic guided-wave structures using SOC/SOL technique in FEM have been presented. After removing the port discontinuities, effective propagation parameters of core periodic structures can be accurately determined. Separately, the HFSS-SOL is proved to have an extremely wide applicability, and FEM-SOC intrinsically owns a remarkable flexibility to implement the feeding structures. Evidently, these two techniques are believed to be highly effective and efficient, which can accurately characterize various kinds of guided-wave structures with periodic configurations.

ACKNOWLEDGMENT

This work was supported in part by the National Natural Science Foundation of China through the General Program under Grant 61571468, in part by the Macao Science and Technology Development Fund through the FDCT Research Grant under Grant 091/2016/A2, in part by the University of Macau through the CPG Research Grant under Grant CPG2017-00028-FST and the Multi-Year Research Grant under Grant MYRG2017-00007-FST.

REFERENCES

[1] F. Xu, K. Wu, and W. Hong, "Domain decomposition FDTD algorithm combined with numerical TL calibration technique and its application in parameter extraction of substrate integrated circuits," *IEEE Trans. Microw. Theory Techn.*, vol. 54, no. 1, pp. 329-338, Jan. 2006.

[2] N. Ranjkesh and M. Shahabadi, "Reduction of dielectric losses in substrate integrated waveguide," *Electron. Lett.*, vol. 42, no. 21, pp. 1230-1231, Oct. 2006.

[3] F. Parment, A. Ghiotto, T. Vuong, J. Duchamp, and K. Wu, "Air-filled substrate integrated waveguide for low-loss and high power-handling millimeter-wave substrate integrated circuits," *IEEE Trans. Microw. Theory Tech.*, vol. 63, no. 4, pp. 1228-1238, Apr. 2015.

[4] N. B.-Makou and A. A. Kishk, "Contactless air-filled substrate integrated waveguide," *IEEE Trans. Microw. Theory Tech*, vol. 66, no. 6, pp. 2928-2935, June 2018.

[5] C. Caloz and T. Itoh, *Electromagnetic Metamaterials: Transmission Line Theory and Microwave Applications*. John Wiley & Sons, IEEE Press, 2005.

[6] R. E. Collin, *Foundation of Microwave Engineering*. 1st ed., New York, USA: McGraw-Hill, 1966.

[7] ANSYS [Online]. Available: https://www.ansys.com

[8] CST Computer Simulation Technology [Online]. Available: http://www.cst.com/

[9] L. Zhu and K. Wu, "Unified equivalent-circuit

model of planar discontinuities suitable for field theory-based CAD and optimization of M(H)MIC's," *IEEE Trans. Microw. Theory Tech.*, vol. 47, no. 9, pp. 1589-1602, Sep. 1999.

[10] J. C. Rautio, "A de-embedding algorithm for electromagnetics," *Int. J. RF Microw. Comput.-Aided Eng.*, vol. 1, no. 3, pp. 282-287, July 1991.

[11] Z. J. Cendes and J.-F. Lee, "The transfinite element method for modeling MMIC devices," *IEEE Trans. Microw. Theory Techn.*, vol. 36, no. 12, pp. 1639-1649, Dec. 1988.

[12] P. Li, L. J. Jiang, Y. J. Zhang, S. Xu, and H. Bagci, "An efficient mode based domain decomposition hybrid 2D/Q-2D finite-element time-domain method for power/ground plate-pair analysis," *IEEE Trans. Microw. Theory Techn.*, vol. 66, no. 10, pp. 4357-4366, Oct. 2018.

[13] P. Li, L. J. Jiang, and H. Bagci, "Transient analysis of dispersive power-ground plate-pairs by DGTD method with wave port excitation," *IEEE Trans. Electromagn. Compat.*, vol. 59, no. 1, pp. 172-183, Feb. 2017.

[14] J. C. Rautio and V. I. Okhmatovski, "Unification of double-delay and SOC electromagnetic de-embedding," *IEEE Trans. Microw. Theory Techn.*, vol. 53, no. 9, pp. 289-292, Sep. 2005.

[15] J. C. Rautio, "Deembedding the effect of a local ground plane in electromagnetic analysis," *IEEE Trans. Microw. Theory Techn.*, vol. 53, no. 2, pp. 770-776, Feb. 2005.

[16] E. D. Caballero, A. Belenguer, H. Esteban, and V. E. Boria, "Thru-reflect-line calibration for substrate integrated waveguide devices with tapered microstrip transitions," *Electron. Lett.*, vol. 49, no. 2, pp. 132-133, Jan. 2013.

[17] X.-P. Chen and K. Wu, "Accurate and efficient design approach of substrate integrated waveguide filter using numerical TRL calibration technique," in *IEEE MTT-S Int. Microw. Symp. Dig.*, pp. 1231-1234, June 2008.

[18] L. Han, K. Wu, X.-P. Chen, and F. He, "Accurate analysis of finite periodic substrate integrated waveguide structures and its applications," in *IEEE MTT-S Int. Microw. Symp. Dig.*, pp. 864-867, May 2010.

[19] K. W. Eccleston, "A new interpretation of through-line (TL) calibration," *IEEE Trans. Microw. Theory and Techn.*, vol. 64, no. 11, pp. 3887-3893, Nov. 2016.

[20] L. Li and K. Wu, "Numerical through-resistor (TR) calibration technique for modeling of microwave integrated circuits," *IEEE Microw. Guided Wave Lett.*, vol. 14, no. 4, pp. 139-141, Apr. 2004.

[21] M. A. Eberspächer and T. F. Eibert, "Dispersion analysis of complex periodic structures by full-wave solution of even-odd-mode excitation problems for single unit cells," *IEEE Trans. Antennas Propag.*, vol. 61, no. 12, pp. 6075-6083, Dec. 2013.

[22] L. Zhu, "Guided-wave characteristics of periodic coplanar waveguides with inductive loading - unit-length transmission parameters," *IEEE Trans. Microw. Theory Tech.*, vol. 51, no. 10, pp. 2133-2138, Oct. 2003.

[23] J. Gao and L. Zhu, "Characterization of infinite- and finite-extent coplanar waveguide metamaterials with varied left- and right-handed passbands," *IEEE Microw. Wireless Comp. Lett.*, vol. 15, no. 11, pp. 805-807, Nov. 2005.

[24] Q.-S. Wu and L. Zhu, "Numerical de-embedding of effective wave impedances of substrate integrated waveguide with varied via-to-via spacings," *IEEE Microw. Wireless Compon. Lett.*, vol. 26, no. 1, pp. 1-3, Jan. 2016.

[25] D. Xie, L. Zhu, and X. Zhang, "An EH_0-mode microstrip leaky-wave antenna with periodical loading of shorting pins," *IEEE Trans. Antennas Propag.*, vol. 65, no. 7, pp. 3419–3426, May. 2017.

[26] L. Zhu, Q.-S. Wu, and S.-W. Wong, "Numerical SOC/SOL calibration technique for de-embedding of periodic guided-wave structures," in *2016 IEEE Int. Conf. on Comput. Electromagn.* (ICCEM), Feb. 2016.

[27] Y. Li, S. Sun, and L. Zhu, "Numerical modeling and de-embedding of non-planar periodic guided-wave structures via short-open calibration in 3-D FEM algorithm," *IEEE Access* (in Press).

[28] Y. Li and L. Zhu, "A short-open calibration method for accurate de-embedding of 3-D non-planar microstrip line structures in finite element method," *IEEE Trans. Microw. Theory Tech.*, vol. 66, no. 3, pp. 1172-1180, Mar. 2018.